Research Article Vol. 29, No. 2 / 18 January 2021 / Optics Express 2458
Optics EXPRESS

Kerr-lens mode-locked Cr:ZnS oscillator reaches the spectral span of an optical octave

SERGEY VASILYEV,[1,*] IGOR MOSKALEV,[1] VIKTOR SMOLSKI,[1] JEREMY PEPPERS,[1] MIKE MIROV,[1] YURY BARNAKOV,[1] VLADIMIR FEDOROV,[1,2] DMITRY MARTYSHKIN,[1,2] SERGEY MIROV,[1,2] AND VALENTIN GAPONTSEV[3]

[1]IPG Photonics – Southeast Technology Center, Birmingham, AL 35211, USA
[2]Department of Physics, University of Alabama at Birmingham, Birmingham, AL 35294, USA
[3]IPG Photonics Corporation, 50 Old Webster Rd, Oxford, MA 01540, USA
[*]svasilyev@ipgphotonics.com

Abstract: We report, to the best of our knowledge, the first super-octave femtosecond polycrystalline Cr:ZnS laser at the central wavelength 2.4 μm. The laser is based on a non-polarizing astigmatic X-folded resonator with normal incidence mounting of the gain element. The chromatic dispersion of the resonator is controlled with a set of dispersive mirrors within one third of an optical octave over 2.05–2.6 μm range. The resonator's optics is highly reflective in the range 1.8–2.9 μm. The components of the oscillator's output spectrum at the wavelengths 1.6 μm and 3.2 μm are detected at –60 dB with respect to the main peak. Average power of few-cycle Kerr-lens mode-locked laser is 1.4 W at the pulse repetition frequency 79 MHz. That corresponds to 22% conversion of cw radiation of Er-doped fiber laser, which we used for optical pumping of the Cr:ZnS oscillator.

1. Introduction

Super-octave femtosecond (fs) sources have special significance in laser science and technology because they enable self-referencing of the optical frequency combs and the carrier-envelope phase measurement of isolated fs pulses via nonlinear f-to-2f interferometry [1,2]. The vast majority of fs lasers have sub-octave spectral bandwidths. Therefore, fs oscillators and amplifiers are often combined with additional stages for nonlinear broadening of pulses' spectra. The generation of super-octave spectra at μJ-level energies of fs pulses is very straightforward: this goal is usually achieved via supercontinuum generation (SCG) in bulk dielectrics and semiconductors [3]. The techniques for nonlinear spectral broadening of unamplified pulse trains from fs oscillators are also well established. These techniques rely on the coupling of pJ-to-nJ pulses, at MHz-to-GHz pulse repetition frequencies (f_R), to specially designed nonlinear fibers and waveguides [4,5,6,7]. Further, there have been a number of recent reports on the generation of octave-spanning continua in structured bulk materials with $\chi^{(2)}$ nonlinearity that occurred at a relatively low energy of fs pulses ($E_P \approx 10$ nJ) and at high repetition frequencies ($f_R \approx 0.1$ GHz) [8,9,10].

Yet most elegant and therefore attractive technique of super-octave lasing is the direct generation of an octave-spanning spectrum in an optical resonator of a mode-locked laser oscillator. An important advantage of this special regime is the possibility to detect and stabilize the oscillator's carrier envelope offset frequency (f_{CEO}) with high precision using simplified f-to-2f interferometry [11,12]. The first super-octave oscillator, based on a combination of dispersive mirrors and prisms, was demonstrated in 2001 [13]. More practical prismless super octave laser designs, including compact $f_R \approx 1$ GHz oscillators were introduced shortly after [14,15,16].

All implementations of super-octave oscillators reported to date are Kerr-lens mode-locked Ti:sapphire laser oscillators equipped with matched pairs of dispersive mirrors [17,18] enabling

#411984 https://doi.org/10.1364/OE.411984
Journal © 2021 Received 14 Oct 2020; revised 21 Dec 2020; accepted 28 Dec 2020; published 14 Jan 2021

Optics EXPRESS

control of the resonator group-delay dispersion (GDD) over a broad spectral range (typically from 0.6 to 1.2 μm). Here we demonstrate an octave spanning oscillator at the central wavelength 2.4 μm based on Cr:ZnS, a laser material that is often referred to as the "Ti:sapphire of the middle-infrared". The remarkable features of the laser design are simplified dispersion control (GDD was compensated within a third of an octave) and high power (1.4 W). We believe that this new avenue for super-octave lasing leads to a number of interesting opportunities for generation and stabilization of optical frequency combs in the middle-infrared (mid-IR).

2. Laser setup and alignment

Cr:ZnS belongs to a large family of transition-metal-doped II-VI semiconductors (TM^{2+}:II-VI, [19,20]). It features room temperature operation over a broad (1.8–3.3 μm) tuning range. An important advantage of Cr:ZnS and its sister material, Cr:ZnSe, is optical pumping by readily available and reliable Er- and Tm- doped fiber lasers with the optical-to-optical conversion efficiencies up to 60%. Cr:ZnS and Cr:ZnSe are available as single crystals and as polycrystals consisting of a multitude of microscopic single crystal grains. The Kerr-lens mode-locked laser regime is supported by both forms [21,22].

The super-octave polycrystalline Cr:ZnS oscillator is based on an optimized commercial few-cycle Kerr-lens mode locked laser. The laser design is described in details in [23,24]. Several examples of broadband sub-octave oscillators based on the same design are provided in [25]. In short, an AR coated 5-mm long polycrystalline Cr:ZnS gain element is mounted at normal incidence in the X-folded standing-wave resonator between two curved mirrors with 100-mm radii and is cooled with a room temperature water. The laser is optically pumped with a radiation of commercial randomly polarized Er- doped fiber laser (EDFL). A part of the fundamental mid-IR laser radiation (f) is converted to second harmonic (2f) via random quasi phase matching process in polycrystalline Cr:ZnS (RQPM, [26]) and partially transmitted trough the right curved mirror.

Dispersion of the resonator was controlled within the spectral bandwidth 2.05–2.6 μm. We relied on the theoretical GDD spectra of the resonator's optics and on the available data on the refractive index of undoped ZnS in order to evaluate the chromatic dispersion of the resonator. According to our estimates, net third-order dispersion (TOD) of the resonator was compensated while net GDD was overcompensated to about –125 fs^2 with the residual GDD oscillations of about ±80fs^2, as illustrated in Fig. 3(a).

The laser was first optimized for maximum cw output power at 6 W of EDFL pump power. The distance between the curved mirrors was then adjusted in order to enable Kerr-lens mode-locking, which was initiated by a mirror translation. The experiments were carried out at an ambient air humidity as will be discussed below.

Important features of this laser design that, we believe, enable robust few-cycle Kerr-lens mode-locking in polycrystalline Cr:ZnS are: (i) normal incidence mounting of the gain element, (ii) use of a nonpolarizing resonator, and (ii) use of output couplers with relatively high transmission (R_{OC} = 50%, in this particular case). Our experience shows that the astigmatism of the resonator is not an impediment for Kerr-lens mode-locking, see, e.g. [27]. Further, the output pulse train is linearly polarized (although it is possible to obtain two pulse trains at two orthogonal polarizations [28]).

Normal incidence mounting of the gain element provided us with additional flexibility for optimization of the laser for shortest pulses by translation of the gain element along the optical axis of the resonator, as described in [22,23]. In this particular case, the optimizations included translations of the gain element along and across the optical axis; adjustments of the pump power and pump focusing; small alignments of the resonator's mirrors.

Optics EXPRESS

3. Experimental results

Spectral parameters of the oscillator before and after optimization are comparted in Fig. 2. Spectra (i) and (ii) were measured after the initial assembly of the oscillator at low and at 50% relative air humidity (RH) inside the optical compartment, respectively (in the former case we purged the oscillator with dry air). As can be seen, an increase of the water vapor content inside the resonator results in a blue shift of the pulses' spectrum (by about 50 nm) as well as in the noticeable change of the spectral distribution. We then carried out several rounds of optimizations – as described in previous section – in order to maximize the spectral bandwidth of output pulses. The final spectrum is shown in Fig. 2 by dashed line. It corresponds to 1.4 W average laser power in mode-locked regime at 6.35 W EDFL pump power. That, in turn, corresponds to 22% conversion of cw EDFL radiation to fs mid-IR pulses. The polarization of the optimized laser was linear and vertical (perpendicular to the plane of Fig. 1) in both cw and Kerr-lens mode-locked laser regimes.

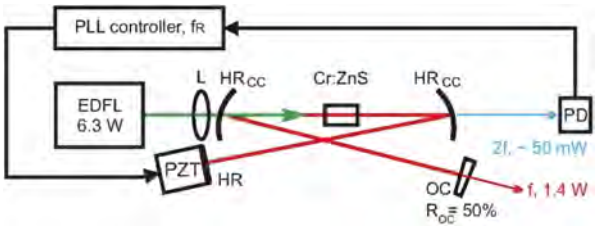

Fig. 1. Laser setup. EDFL, Er- doped fiber laser at the wavelength 1567 nm; L, plano-convex lens with f = 80 mm; HR and HR_{CC}, plane and concave mid-IR high reflectors, respectively; OC, output coupler. Pump beam is focused in Cr:ZnS gain element with ≈60 μm $1/e^2$ intensity diameter. The length of the optical resonator is controlled with a piezo (PZT). The f_R is measured at second harmonic wavelength (2f) with an InGaAs detector (PD). Detected rf signal is fed to the phase-locking electronics. For simplicity, only the end mirrors HR and OC are shown in the resonator; the other four HR mirrors are used to fold the laser beams for footprint reduction. The resonator's length is about 1.9 m (f_R = 79.06 MHz)

Importantly, the broadest spectrum of pulses was obtained at high RH (52–55% at about 20–22°C). We believe that the water vapor in the laser resonator has served as a means for fine-tuning of the resonator's chromatic dispersion. On the one hand, our experiments show that the fine-tuning of a Cr:ZnS oscillator via the RH variation is a reproducible technique (see, e.g., Fig. 4(c) in [29]). On the other hand, the RH controllers are slow and cumbersome devices. Therefore, the practical applications of few-cycle Cr:ZnS oscillators require the development of more convenient tuning methods (e.g. a fine-tuning with the intracavity wedges made of appropriate IR materials).

The obtained output spectrum of the optimized oscillator, measured with a high dynamic range, is illustrated in Fig. 3(b). The spectrum is compared with net reflectivity of the high reflectors, net-GDD of the resonator, and with air transmission in 2-m long optical path, as shown in Fig. 3(a).

The obtained spectrum of output pulses spans 350 nm (20 THz) at half maximum, 740 nm (42 THz) at –10 dB and an optical octave 1600 nm (94 THz) at –60 dB with respect to the main peak. We explain very low level of the optical signal at the wings of the spectrum by significant losses at sub-octave high-reflectors (see Fig. 3(a)). Further, a broad super-octave spectral span is obtained with an unusually narrow, one third of an octave, dispersion control bandwidth. Therefore, the conventional soliton like pulse propagation in the resonator cannot explain the shaping of the spectrum. It is likely that circulating pulse acquires significant additional spectral broadening during a single pass through a highly nonlinear polycrystalline Cr:ZnS medium.

Optics EXPRESS

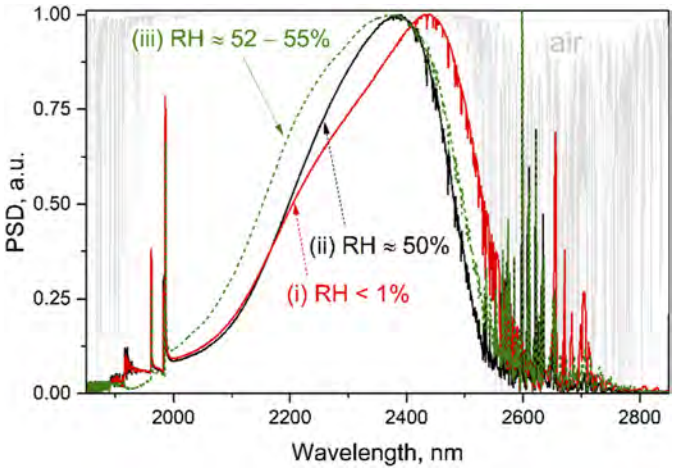

Fig. 2. Spectra of the oscillator before (i, ii, solid lines) and after (iii, dashed line) fine tuning. Spectra (i) and (ii). were acquired with low dynamic range (SNR ≈ 20 dB) using a Thorlabs OSA207C Fourier-transform optical spectrum analyzer. Spectrum (iii) was acquired with high dynamic range (see main text). Gray background shows transmission of standard air (HITRAN simulation). A ~1.5 m long optical path between the oscillator's output window and the spectrometer was at standard RH during all measurements.

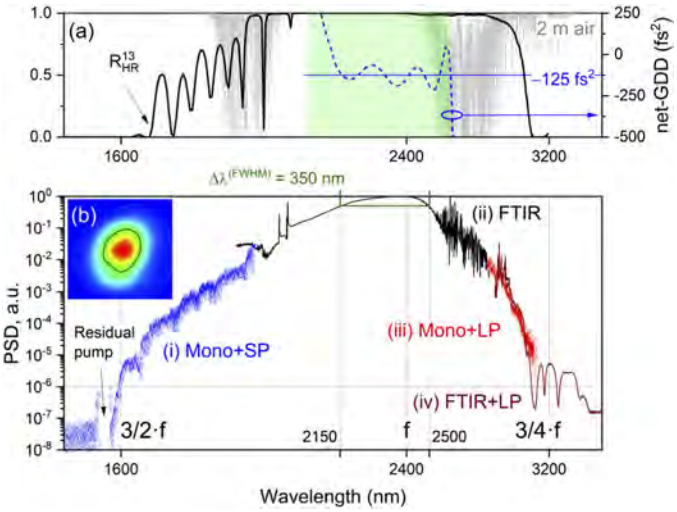

Fig. 3. (a) Solid line, net reflectivity of the resonator's high reflectors (13 bounces in total, theoretical estimate); green rectangle dispersion control bandwidth (see main text); dashed line (right vertical axis), net GDD of the resonator within the dispersion control bandwidth (theoretical estimate); gray background, transmission of standard air in 2 m long resonator (HITRAN simulation). (b) Spectrum of optimized oscillator measured at RH = 52% and presented in log scale. Curves (i) and (iii) were acquired with an Acton Research monochromator using appropriate gratings, detectors and spectral filters. Curves (ii) and (iv) were acquired with a Thorlabs OSA205C-HS Fourier-transform optical spectrum analyzer without filter (ii) and with a long-pass filter (iv). Obtained spectra were then stitched. Insert shows measured beam profile where the solid line marks 50% level with respect to the maximum.

Optics EXPRESS

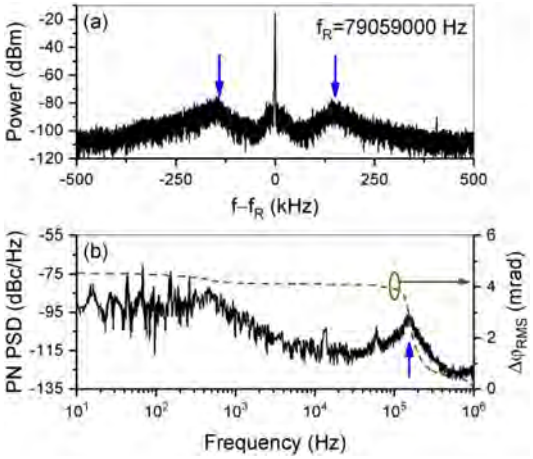

Fig. 4. (a) In-loop rf spectrum of the oscillator with phase-locked f_R measured with 1 kHz resolution bandwidth. (b) Phase noise PSD (solid curves) and accumulated phase error of the signal (dashed curve, integrated from 10 to 10^6 Hz). Vertical arrows show the contributions due to the relative intensity noise of EDFL pump laser. Measurements were carried out with an Aeroflex 3251 rf spectrum analyzer.

Indeed, intracavity pulse energy of 35 nJ allows us to estimate intracavity peak power of 1.5 MW (assuming 20 fs pulses, see discussion below) that significantly exceeds the critical power for self-focusing in Cr:ZnS (about 0.5 MW). In this respect the obtained laser regime has similarities with the regime reported in [14] where the super-octave spectrum at –50 dB level with respect to the main peak was achieved with dispersion control over 3/8 of an octave. We can also point out that the significant nonlinear broadening and generation of super-octave mid-IR spectra (at –40 dB level with respect to the central peak) was observed in a single-pass polycrystalline Cr:ZnS amplifier [10].

Another unusual feature of the implemented super-octave Cr:ZnS oscillator is the robustness of Kerr-lens mode-locking at rather high levels of water vapor absorption inside the resonator, as shown in Fig. 3(a). Temporal stability of obtained pulse train was characterized using the auxiliary near IR 2f output of the laser. The pulse train was detected with a fast InGaAs photodetector (TimeBase PD-1800). We then used a commercial phase locked loop controller to phase-lock the detected signal to a radio frequency (rf) reference as illustrated in Fig. 1. The results of this experiment are summarized in Fig. 4.

The integrated phase noise of the oscillator with phase-locked f_R is 4.4 mrads that corresponds to a timing jitter of about 10 ps. Significant fraction of the phase noise in the fs pulse train arises from the relaxation resonance of EDFL at the frequency 130 kHz. The couplings of the relative intensity noise (RIN) of the EDLF pump to the fs pulse train are marked in Fig. 4 by vertical arrows. Thus, in terms of the pulse train temporal purity, our super-octave oscillator is comparable with other types of few-cycle Kerr-lens mode-locked Cr:ZnS and Cr:ZnSe lasers [30,31].

The pulse width ($\Delta\tau$) of the oscillator was characterized with a custom a 2nd order, two-photon detection interferometric autocorrelator with 20 fs measurement capacity, developed by APE. We used a set of 3 dichroic mirrors to suppress the residual 2f signal in the mid-IR output of the oscillator. We relied on the autocorrelator's control software and used sech^2 fit of the autocorrelation functions for evaluations of the pulse width. Figure 5 compares measured autocorrelation traces with the simulations. The obtained mid-IR spectrum supports 20 fs (2.5-cycle) pulses. An autocorrelation derived from the spectrum is shown in Fig. 5(a). These

Optics EXPRESS

pulses are short enough to acquire a significant temporal broadening during their propagation through a substrate of the output coupler: 1.75 mm thick undoped YAG with GDD ≈ –300 fs^2 ≈ 17^2 fs^2. The acquired chirp can be compensated with a plane parallel plate made of the material with the opposite sign of GDD in the mid-IR spectral range, e.g. a 1-mm thick ZnSe plate. An autocorrelation derived for such a de-chirped pulse is shown in Fig. 5(b). According to the simulation, pulses can be recompressed to about 25 fs (3-cycle) with the residual temporal broadening of 25% due to the uncompensated TOD of the output coupler and of the de-chirping plate (combined TOD ≈ 2000 fs^3 ≈ 12^3 fs^3).

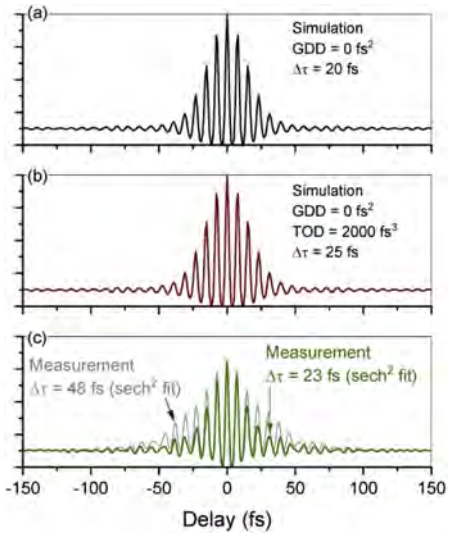

Fig. 5. Interferometric autocorrelation traces (IACs) of output pulses: (a) derived from measured spectrum assuming flat spectral phase; (b) derived from measured spectrum assuming a chirp introduced by 1.75 mm YAG plate and 1 mm ZnSe plate; (c) solid line, IAC measured with 1 mm ZnSe compensation plate; dotted line, IAC measured directly behind the output coupler. In parts (a) and (b) pulse widths are defined at FWHM of the power distributions. In part (c) pulse widths are derived from the IACs using $sech^2$ fit.

As can be seen from Fig. 5(c), the obtained experimental results are in good agreement with the simulations. The IAC measured behind the OC corresponds to chirped pulses with Δτ of about 48 fs. Introduction of the 1-mm ZnSe plate compressed pulses to about 23 fs. Thus, we can estimate 3-cycle output pulses with 17.6 nJ energy and approximately 0.7 MW peak power at the f_R = 79 MHz.

4. Conclusions

In conclusion we demonstrate first Cr:ZnS fs oscillator with an octave-spanning spectrum at the central wavelength 2.4 μm. This significant milestone in the mid-IR laser technology has been reached by a number of improvements in the standard Kerr-lens mode-locked polycrystalline Cr:ZnS laser. Obtained results demonstrate two important features of polycrystalline Cr:ZnS and, most likely, Cr:ZnSe lasers. First and foremost, very broad spectral spans can be obtained in the oscillators with relaxed requirements to the dispersion control of the optical resonator. Further, the mid-IR pulse trains with relatively low timing jitter can be obtained at relatively high levels of water vapor absorption in the resonators of Kerr-lens mode-locked lasers. These features greatly simplify the alignment and the practical applications of the super-octave mid-IR laser oscillators.

Optics EXPRESS

We expect that the use of now available ultra-broadband multilayer coatings for the mid-IR range 2 –3 μm [32] will allow to increase the levels of the optical signal at the wings of the super-octave spectrum by 1–2 orders of magnitude. This, in turn, will enable straightforward measurements of the oscillator's f_{CEO} via monolithic f-to-2f interferometry [11]. An additional set of interesting opportunities is provided by nonlinear frequency conversion directly in the polycrystalline gain elements of super-octave Cr:ZnS (and Cr:ZnSe) lasers. RQPM process in polycrystals is exceptionally broadband and, hence, enables a multitude of intrapulse three-wave mixings [10] as well as the nonlinear mixings between generated fs pulses and pump radiation [23].

Funding. National Institute of Environmental Health Sciences (P42ES027723); U.S. Department of Energy (DE-SC0018378).

Acknowledgments. We thank Michelle Sander with Boston University for valuable discussions and Natasha Antanaitis with Thorlabs for equipment loans. S. M., V. F., and D. M. acknowledge funding from the Department of Energy (DOE), grant number DE-SC0018378 and National Institute of Environmental Health Sciences (NIEHS), grant number P42ES027723.

Disclosures. S. M., V. F., and D. M. declare competing financial interests.

References

1. D. J. Jones, S. A. Diddams, J. K. Ranka, A. Stentz, R. S. Windeler, J. L. Hall, and S. T. Cundiff, "Carrier-envelope phase control of femtosecond mode-locked lasers and direct optical frequency synthesis," Science **288**(5466), 635–639 (2000).
2. A. Baltuska, M. Uiberacker, E. Goulielmakis, R. Kienberger, V. S. Yakovlev, T. Udem, T. W. Hansch, and F. Krausz, "Phase-controlled amplification of few-cycle laser pulses," IEEE J. Sel. Top. Quantum Electron. **9**(4), 972–989 (2003).
3. A. Dubietis, G. Tamošauskas, R. Šuminas, V. Jukna, and A. Couairon, "Ultrafast supercontinuum generation in bulk condensed media," Lith. J. Phys. **57**(3), 113–157 (2017).
4. J. M. Dudley, G. Genty, and S. Coen, "Supercontinuum generation in photonic crystal fiber," Rev. Mod. Phys. **78**(4), 1135–1184 (2006).
5. N. Nagl, K. F. Mak, Q. Wang, V. Pervak, F. Krausz, and O. Pronin, "Efficient femtosecond mid-infrared generation based on a Cr:ZnS oscillator and step-index fluoride fibers," Opt. Lett. **44**(10), 2390–2393 (2019).
6. S. Xie, N. Tolstik, J. C. Travers, E. Sorokin, C. Caillaud, J. Troles, P. S. J. Russell, and I. T. Sorokina, "Coherent octave-spanning mid-infrared supercontinuum generated in As_2S_3-silica double-nanospike waveguide pumped by femtosecond Cr:ZnS laser," Opt. Express **24**(11), 12406–12413 (2016).
7. Y. Okawachi, M. Yu, J. Cardenas, X. Ji, A. Klenner, M. Lipson, and A. L. Gaeta, "Carrier envelope offset detection via simultaneous supercontinuum and second-harmonic generation in a silicon nitride waveguide," Opt. Lett. **43**(19), 4627–4630 (2018).
8. M. Rutkauskas, A. Srivastava, and D. T. Reid, "Supercontinuum generation in orientation-patterned gallium phosphide," Optica **7**(2), 172–175 (2020).
9. A. J. Lind, A. Kowligy, H. Timmers, F. C. Cruz, N. Nader, M. C. Silfies, T. K. Allison, and S. A. Diddams, "Mid-Infrared Frequency Comb Generation and Spectroscopy with Few-Cycle Pulses and $\chi^{(2)}$ Nonlinear Optics," Phys. Rev. Lett. **124**(13), 133904 (2020).
10. S. Vasilyev, I. Moskalev, V. Smolski, J. Peppers, M. Mirov, V. Fedorov, D. Martyshkin, S. Mirov, and V. Gapontsev, "Octave-spanning Cr:ZnS femtosecond laser with intrinsic nonlinear interferometry," Optica **6**(2), 126–127 (2019).
11. H. M. Crespo, J. R. Birge, E. L. Falcão-Filho, M. Y. Sander, A. Benedick, and F. X. Kärtner, "Nonintrusive phase stabilization of sub-two-cycle pulses from a prismless octave-spanning Ti:sapphire laser," Opt. Lett. **33**(8), 833–835 (2008).
12. T. M. Fortier, A. Bartels, and S. A. Diddams, "Octave-spanning Ti:sapphire laser with a repetition rate >1 GHz for optical frequency measurements and comparisons," Opt. Lett. **31**(7), 1011–1013 (2006).
13. R. Ell, U. Morgner, F. X. Kärtner, J. G. Fujimoto, E. P. Ippen, V. Scheuer, G. Angelow, T. Tschudi, M. J. Lederer, A. Boiko, and B. Luther-Davies, "Generation of 5-fs pulses and octave-spanning spectra directly from a Ti:sapphire laser," Opt. Lett. **26**(6), 373–375 (2001).
14. A. Bartels and H. Kurz, "Generation of a broadband continuum by a Ti:sapphire femtosecond oscillator with a 1-GHz repetition rate," Opt. Lett. **27**(20), 1839–1841 (2002).
15. L. Matos, D. Kleppner, O. Kuzucu, T. R. Schibli, J. Kim, E. P. Ippen, and F. X. Kärtner, "Direct frequency comb generation from an octave-spanning, prismless Ti:sapphire laser," Opt. Lett. **29**(14), 1683–1685 (2004).
16. L.-J. Chen, A. J. Benedick, J. R. Birge, M. Y. Sander, and F. X. Kärtner, "Octave-spanning, dual-output 2.166 GHz Ti:sapphire laser," Opt. Express **16**(25), 20699–20705 (2008).
17. O. Razskazovskaya, F. Krausz, and V. Pervak, "Multilayer coatings for femto- and attosecond technology," Optica **4**(1), 129–138 (2017).

Optics EXPRESS

18. S.-H. Chia, G. Cirmi, S. Fang, G. M. Rossi, O. D. Mücke, and F. X. Kärtner, "Two-octave-spanning dispersion-controlled precision optics for sub-optical-cycle waveform synthesizers," Optica **1**(5), 315–322 (2014).
19. L. D. DeLoach, R. H. Page, G. D. Wilke, S. A. Payne, and W. F. Krupke, "Transition metal-doped zinc chalcogenides: Spectroscopy and laser demonstration of a new of gain media," IEEE J. Quantum Electron. **32**(6), 885–895 (1996).
20. S. Mirov, I. Moskalev, S. Vasilyev, V. Smolski, V. Fedorov, D. Martyshkin, J. Peppers, M. Mirov, A. Dergachev, and V. Gapontsev, "Frontiers of mid-IR lasers based on transition metal doped chalcogenides," IEEE J. Sel. Top. Quantum Electron. **24**(5), 1–29 (2018).
21. M. N. Cizmeciyan, H. Cankaya, A. Kurt, and A. Sennaroglu, "Kerr-lens mode-locked femtosecond Cr^{2+}:ZnSe laser at 2420 nm," Opt. Lett. **34**(20), 3056–3058 (2009).
22. S. Vasilyev, M. Mirov, and V. Gapontsev, "Kerr-lens mode-locked femtosecond polycrystalline Cr^{2+}:ZnS and Cr2+ :ZnSe lasers," Opt. Express **22**(5), 5118–5123 (2014).
23. S. Mirov, V. Fedorov, D. Martyshkin, I. Moskalev, M. Mirov, and S. Vasilyev, "Progress in Mid-IR Lasers Based on Cr and Fe Doped II-VI Chalcogenides," IEEE J. Sel. Top. Quantum Electron. **21**(1), 292–310 (2015).
24. S. Vasilyev, I. Moskalev, M. Mirov, S. Mirov, and V. Gapontsev, "Three optical cycle mid-IR Kerr-lens mode-locked polycrystalline Cr^{2+}:ZnS laser," Opt. Lett. **40**(21), 5054–5057 (2015).
25. S. Vasilyev, I. Moskalev, M. Mirov, V. Smolski, S. Mirov, and V. Gapontsev, "Ultrafast middle-IR lasers and amplifiers based on polycrystalline Cr:ZnS and Cr:ZnSe," Opt. Mater. Express **7**(7), 2636–2650 (2017).
26. S. Vasilyev, I. Moskalev, M. Mirov, V. Smolski, S. Mirov, and V. Gapontsev, "Mid-IR Kerr-lens mode-locked polycrystalline Cr:ZnS and Cr:ZnSe lasers with intracavity frequency conversion via random quasi-phase-matching," Proc. SPIE **9731**, 97310B (2016).
27. S. Vasilyev, I. Moskalev, M. Mirov, V. Smolski, S. Mirov, and V. Gapontsev, "Kerr-Lens Mode-Locked Middle IR Polycrystalline Cr:ZnS Laser with a Repetition Rate 1.2 GHz," in *Lasers Congress 2016 (ASSL, LSC, LAC)*, OSA Technical Digest (online) (Optical Society of America, 2016), paper AW1A.2
28. D. Martyshkin, V. Fedorov, T. Kesterson, S. Vasilyev, H. Guo, J. Liu, W. Weng, K. Vodopyanov, T. J. Kippenberg, and S. Mirov, "Visible-near-middle infrared spanning supercontinuum generation in a silicon nitride (Si_3N_4) waveguide," Opt. Mater. Express **9**(6), 2553–2559 (2019).
29. S. Vasilyev, V. Smolski, J. Peppers, I. Moskalev, M. Mirov, Y. Barnakov, S. Mirov, and V. Gapontsev, "Middle-IR frequency comb based on Cr:ZnS laser," Opt. Express **27**(24), 35079–35087 (2019).
30. Y. Wang, T. T. Fernandez, N. Coluccelli, A. Gambetta, P. Laporta, and G. Galzerano, "47-fs Kerr-lens mode-locked Cr:ZnSe laser with high spectral purity," Opt. Express **25**(21), 25193–25200 (2017).
31. N. Nagl, S. Gröbmeyer, V. Pervak, F. Krausz, O. Pronin, and F. K. Mak, "Directly diode-pumped, Kerr-lens mode-locked, few-cycle Cr:ZnSe oscillator," Opt. Express **27**(17), 24445–24454 (2019).
32. V. Pervak, T. Amotchkina, Q. Wang, O. Pronin, K. F. Mak, and M. Trubetskov, "2/3 octave Si/SiO_2 infrared dispersive mirrors open new horizons in ultrafast multilayer optics," Opt. Express **27**(1), 55–62 (2019).